Stability of gold cages (Au_{16} and Au_{17}) at finite temperature

PRACHI CHANDRACHUD[1], KAVITA JOSHI[2], SAILAJA KRISHNAMURTY[2] and D G KANHERE[1,2,*]

[1]Department of Physics, University of Pune, Ganeshkhind, Pune 411 007, India
[2]Centre for Modelling and Simulation, University of Pune, Ganeshkhind, Pune 411 007, India
*Corresponding author
E-mail: kanhere@unipune.ernet.in; prachiavi@gmail.com

Abstract. We have employed *ab initio* molecular dynamics to investigate the stability of the smallest gold cages, namely Au_{16} and Au_{17}, at finite temperatures. First, we obtain the ground state structure along with at least 50 distinct isomers for both the clusters. This is followed by the finite temperature simulations of these clusters. Each cluster is maintained at 12 different temperatures for a time period of at least 150 ps. Thus, the total simulation time is of the order of 2.4 ns for each cluster. We observe that the cages are stable at least up to 850 K. Although both clusters melt around the same temperature, i.e. around 900 K, Au_{17} shows a peak in the heat capacity curve in contrast to the broad peak seen for Au_{16}.

Keywords. Thermodynamics of clusters; gold clusters; density functional theory.

PACS Nos   31.15.Ar; 31.15.es; 31.15.xv; 36.40.Qv

1. Introduction

In recent years gold nanoparticles have attracted much attention due to their vital role in nanoscale electronic, optical and medical diagnostic devices [1,2]. For example, small clusters of gold have attracted interest as tips and contacts in molecular electronic circuits [3]. One of the interesting application of these clusters is in the area of catalysis. Gold in its bulk form is known to be a noble metal. But, gold in nanoregime has shown size-sensitive reactive properties and is considered to be a promising chemical catalyst [4–6]. Owing to such potential applications, a large amount of experimental [7–11] and theoretical [12–20] work probing structural and electronic properties of Au clusters has been reported. These reports reveal that the ground state (GS) geometries of gold clusters with sizes up to a few tens of atoms exhibit interesting and strikingly different trends. These undergo a very interesting structural evolution. There has been a debate about the size at which the planar to

non-planar transition occurs [21–24]. A very recent experimental evidence of hollow cage structures [18] (for $n = 16, 17, 18$) analogous to C_{60} has generated an excitement and focussed interest on gold clusters in this size range. Such hollow cages are predicted for larger sizes as well [25,26] which opens up new possibilities of encapsulating impurities like transition metal atoms for tuning their properties [27,28]. Almost all the studies reported so far on these cages pertain to zero temperature properties. Since the realistic applications are at finite temperatures, typically at room temperature and above, it is of considerable importance to investigate their stability and other properties at finite temperatures. In the present work we investigate the finite temperature behaviour of two clusters, namely Au_{16} and Au_{17}, using *ab initio* method.

Finite temperature investigations of small clusters have brought out many interesting and at times counterintuitive facts [29–35]. In nanoregime, there are two scales, the first one consists of a few hundreds to few thousands of atoms where the properties such as melting temperature show the expected monotonic trend as a function of size of the cluster. However, in the size range of few tens to few hundreds of atoms the details of the electronic structure and the ground state geometry which could be quite different from the bulk can have significant influence on finite temperature properties. This has been demonstrated experimentally in the case of melting temperatures of Na clusters with size between 55 and 357 atoms [29]. Na clusters show depression in the melting temperature (T_m) which was consistent with the common sense understanding that clusters having higher surface-to-volume ratio will melt at lower temperatures. Rather counterintuitive observation was made in the case of Sn and Ga clusters, that these clusters melt at higher than bulk temperatures [32,33]. The finite temperature simulations of these clusters demonstrated that change in the nature of bonding is responsible for the elevated T_m [36]. More intriguing and somewhat less understood observations concern size-sensitive melting behaviour of small clusters of Ga and Al [34,35]. It has been observed that the addition of a few atoms can change the melting temperature as well as shape of the heat capacity curve dramatically. It has been demonstrated that 'ordered' ground state structure results into a well-defined melting peak [37–42].

There have been a few calculations reported on the finite temperature behaviour of small gold clusters with classical molecular dynamics (MD) using parametrized potentials like Voter-Chen [43,44]. However, these potentials are based on two-body or three-body interactions and fall short of mimicking the real scenario of many interacting electrons and ions. On the other hand, simulating finite temperature behaviour with *ab initio* method is computationally very expensive. To the best of our knowledge, there are only two *ab initio* simulations reported so far. Soulé *et al* have simulated finite temperature behaviour of gold clusters with 7, 13 and 20 atoms [45]. Krishnamurty *et al* carried out extensive first principles MD simulations to investigate finite temperature behaviour of Au_{19} and Au_{20} [39]. The ground state geometry of Au_{19} is the same as that of Au_{20} except for the missing corner atom of the pyramid. Both the clusters melt around 780 K, a temperature much below the bulk melting temperature. However, Au_{19} undergoes a vacancy-assisted melting transition leading to a broad peak in the heat capacity curve whereas Au_{20} with a symmetric ground state has a well-defined peak in the heat capacity curve.

In the present work we have investigated the stability of Au_{16} and Au_{17} gold cages at finite temperatures. These are the smallest cages of gold clusters found so far. The capacity of these clusters to hold an atom inside the cage makes them technologically very interesting. The isomer distribution of these clusters reveals that the isomers of Au_{17} are more symmetric than those of Au_{16}. Further, the isomer energy distribution of Au_{16} is continuous whereas that of Au_{17} shows gaps. Our simulations indicate that these cages are stable up to at least 850 K with Au_{17} having a noticeable peak in the heat capacity curve and Au_{16} with a broad transition region. In §2 we briefly discuss the computational details. Results and discussion are presented in §3. We conclude with summary in §4.

2. Computational details

All the calculations have been performed within the framework of *ab initio* density functional theory (DFT). We have employed the plane-wave method where the core-valence interactions are described using Vanderbilt's ultrasoft pseudo-potentials [46] as implemented in the VASP package [47]. It may be noted that pseudo-potentials used in the plane-wave method incorporate the relativistic effects. For the purpose of calculating the equilibrium geometries, we have used generalized gradient approximation (GGA). The calculations have been carried out in two steps. In the first step we have obtained 50 distinct isomers for both the clusters. In order to get many distinct initial configurations for geometry optimization, constant temperature Born–Oppenheimer molecular dynamics (BOMD) runs were carried out at four different temperatures 300, 600, 900 and 1200 K each with a time-scale of 60 ps. Around 150 configurations were chosen from these initial runs by examining the potential energy as a function of time. The resulting isomers after minimization were examined visually as well as by carrying out the nearest-neighbour bond length analysis so as to obtain geometrically distinct structures by removing the duplicates.

Next, for calculating the heat capacities, BOMD simulations have been carried out for 14 different temperatures in the range of 200 to 2000 K for Au_{16} and 12 temperatures in the range of 200 to 1600 K for Au_{17}. Each cluster is maintained at each temperature for a time period of at least 150 ps using Nośe thermostat [48]. For each of the temperature first 30 ps of data are discarded for thermalization. Thus, the total simulation time is around 2.4 ns. An energy cut-off of 179.7 eV is used for the plane-wave expansion of the wave function. We have used a convergence of 10^{-4} eV in the total energy during the self-consistency. The size of the simulation box is chosen to be 20 Å which is found to be sufficient for the energy convergence. The data are used to calculate the ionic specific heat of each cluster using multiple histogram method (MH) [49–51]. The calculation of the heat capacity using the MH technique is sensitive to the number of temperatures at which the thermodynamic behaviour of the cluster is simulated. The range and the number of temperatures are chosen to ensure an adequate overlap of the potential energy distribution. The MH method extracts the classical ionic density of states $\Omega_C(E)$ of the cluster, or equivalently the classical ionic entropy $S(E) = k_B \ln \Omega_C(E)$, from the simulation data. With $S(E)$ in hand, one can calculate the thermodynamic averages in a variety of ensembles [52].

We have also calculated the mean square displacements (MSD), an important parameter for monitoring the phase change which is defined as

$$\langle \mathbf{R}^2(t) \rangle = \frac{1}{MN} \sum_{m=1}^{M} \sum_{I=1}^{N} \left[\mathbf{R}_I(t_{0m} + t) - \mathbf{R}_I(t_{0m}) \right]^2, \tag{1}$$

where N is the number of atoms in the system and $\mathbf{R}_I$ is the position of the Ith atom and we average over M different time origins (t_{0m}) spanning the entire trajectory. The MSD of the cluster indicates the displacement of the ions with respect to their original positions as a function of time. Thus, one expects MSD to converge to the square of the radius of the cluster when the system is in liquid-like region.

We have also calculated the radial distribution function $[g(r)]$. It is defined as the average number of atoms within the region r and $r + \mathrm{d}r$ from the centre of mass of the cluster. The radial distribution function for a symmetric cluster will exhibit distinct peaks at low temperatures corresponding to different shells. With increasing temperature these peaks are expected to broaden due to oscillatory motion of ions. Eventually, at high temperatures, there will be a merger of these peaks indicating the diffusive motion of ions.

3. Results and discussion

We begin our discussion by noting the ground state geometries and some low-lying isomers of Au_{16} and Au_{17} which are shown in figures 1 and 2 respectively. It may be pointed out that the ground state of Au_{16} and Au_{16}^- have been reported and are known to be different from each other [18,19]. The ground state geometry of neutral cluster is a symmetric flat cage while that of anionic cluster is a hollow cage. Our results agree with those reported in the literature. Since the isomers at various energies are relevant to the finite temperature analysis, we have analysed about 50 distinct isomers within the energy range of 0.4 eV above the ground state energy. These isomers can be approximately grouped into three categories. The low energy isomers (within 0.1 eV with respect to the ground state) are characterized by the flat cage structures [19] (figures 1a–1c). These structures differ from the ground state with respect to their base and capping. The next in the energy scale (from 0.11 to 0.15 eV with respect to the ground state) are the hollow cages which are characterized by the existence of two six-membered distorted rings arranged nearly parallel to each other (figures 1d and 1e). These rings give rise to a hollow cage-like structure. Typically, these structures do not display any definite symmetry and once again the isomers in this class differ by the nature of the caps on these rings and small distortions. Lastly, still higher in the energy scale (above 0.16 eV with respect to the ground state) are the intermediate structures between the above two as shown in figures 1f–1h. Most of these have only one five- or six-membered ring. We also note the existence of a highly symmetric hollow cage (figure 1i) which is known to be the ground state of Au_{16}^-. This isomer has an energy which is about 0.35 eV higher with respect to the ground state. Indeed this isomer is observed in our simulations at around 850 K. Another significant characteristic of these isomers is their energy distribution which turns out to be almost continuous. We will discuss

(a) 0.000 eV   (b) 0.088 eV   (c) 0.100 eV

(d) 0.138 eV   (e) 0.149 eV   (f) 0.192 eV
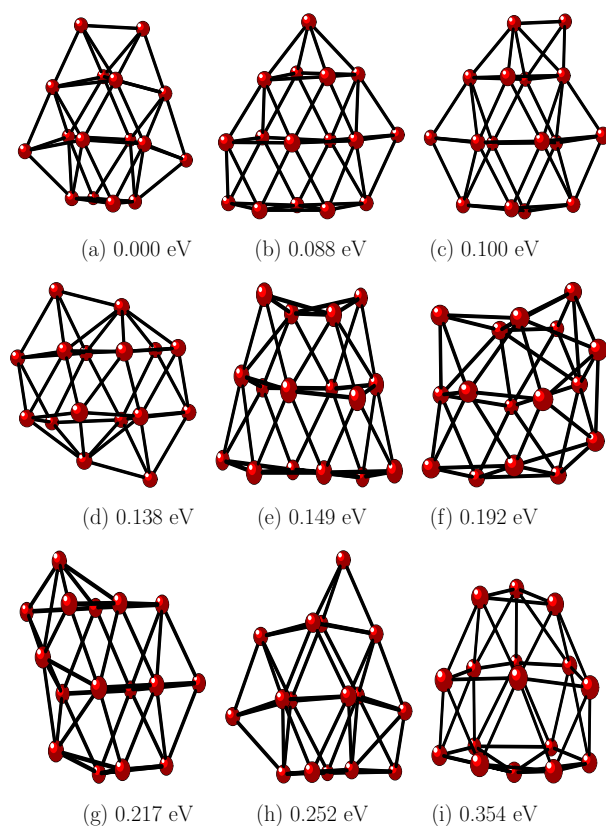
(g) 0.217 eV   (h) 0.252 eV   (i) 0.354 eV

Figure 1. The ground state geometries and various isomers of Au_{16}. The numbers correspond to the difference in the energy with respect to the ground state.

its possible effect on the nature of the heat capacity curve and contrast its behaviour with that of Au_{17}.

In contrast to Au_{16}, the ground state of Au_{17} exhibits a hollow cage structure [19]. In fact there are two nearly degenerate geometries (very close in energy $\approx$0.01 eV) which are the probable candidates for the ground state as shown in figures 2a and 2b respectively. While one of the structures has two pentagons stacked over each other and three distinct atomic caps, the other one has a six-membered ring at the centre. Figures 2c and 2d show the next low-lying isomers which are also hollow cages higher in energy by 0.07 eV. In figure 2e we show a caged structure which is slightly distorted while figures 2f and 2g represent high energy cages with energy around 0.35 eV. Interestingly, none of the structures discussed so far have a gold atom trapped inside. In figure 2h a high energy isomer with such a trapped atom is seen. This isomer occurs at 0.47 eV higher in energy with respect to the lowest energy structure. The noteworthy point is that the isomers even up to a typical energy of 0.35 eV consist of predominantly hollow cages, either symmetric or distorted.
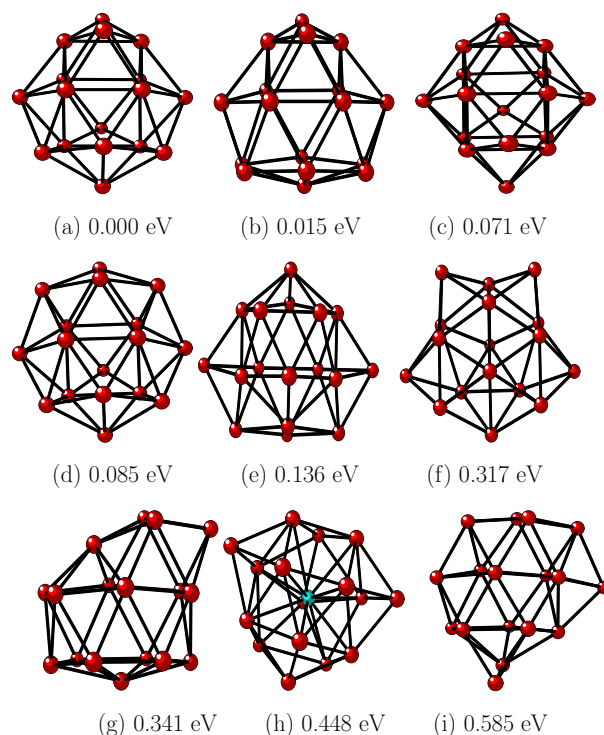
(a) 0.000 eV   (b) 0.015 eV   (c) 0.071 eV

(d) 0.085 eV   (e) 0.136 eV   (f) 0.317 eV

(g) 0.341 eV   (h) 0.448 eV   (i) 0.585 eV

Figure 2. The ground state geometries and various isomers of Au_{17}. The numbers correspond to the difference in the energy with respect to the ground state.

We now present the calculated ionic specific heats in figure 3. It is clear from the figure that both Au_{16} and Au_{17} show a rather broad heat capacity curve with some notable differences. Au_{16} shows solid-to-liquid transition from 600 to 1000 K. In contrast, Au_{17} shows a weak shoulder at 500 K and a noticeable peak at 900 K. This peak may be identified as the melting peak. Typically in the finite size systems, melting temperature is not sharp. At low temperatures, it is easy to characterize the cluster as solid-like, where the atoms execute small oscillatory motion. In this region MSDs are small. The other extreme is the liquid-like state where there is a clear diffusive motion of the atoms throughout the cluster. The MSDs in this region are of the order of square of the radius of the cluster and tend to saturate. The transition region around the melting peak cannot be definitely characterized as solid-like or liquid-like. In general, as the temperature increases, the pre-melting features can occur due to the isomerization or in some cases surface melting.

In order to make a detailed analysis of the ionic motion we examine the atomic trajectories in the form of movies. It is observed that at low temperatures (up to 400 K), Au_{16} cluster is seen to visit the first isomer (figure 1b) quite frequently. Further, up to 600 K, in addition to the first isomer, the next low energy structures (figures 1c and 1d) are also observed. Thus, up to this temperature the cluster moves through either flat or hollow caged isomers. Around 700 K, the cage pattern
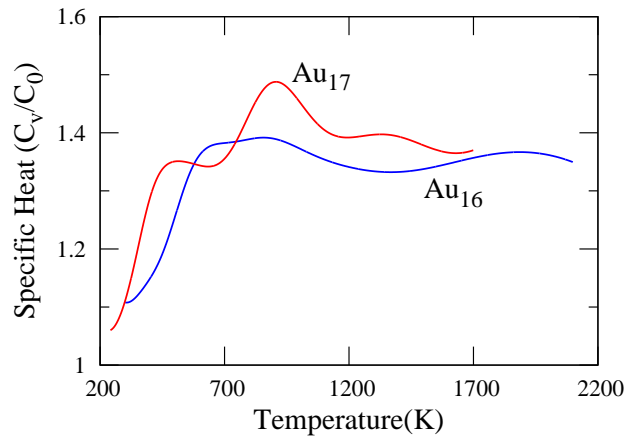
Figure 3. Normalized specific heat curve for Au$_{16}$ and Au$_{17}$.
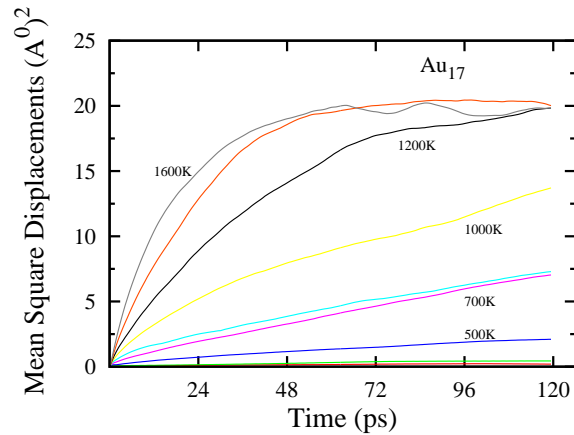

Figure 4. Mean square displacements of Au$_{17}$ over 120 ps.

is seen to be disturbed and a diffusive motion of the atoms results in a high energy distorted flat cage structure (figure 1h). Such distortions are retained till 900 K above which the cluster is seen to melt. Thus, from 600 K onwards the movie reveals that the cluster is dominated by isomerization from flat cages to hollow ones and again to distorted flat type. The process continues even above the melting temperature.

For Au$_{17}$, a weak shoulder at 500 K can be attributed to isomerization. Up to 800 K, the shape of the cluster remains more or less cage-like in spite of distortions. However, we do not observe a complete destruction of the cage. The motion clearly indicates the dominance of isomers in the sense that at least up to 1000 K many isomers belonging to hollow or distorted type of cages are observed. It is only above 1000 K or so, we observe the open structures and consequently, complete destruction of cages. Indeed, around this temperature the MSDs reach the value of
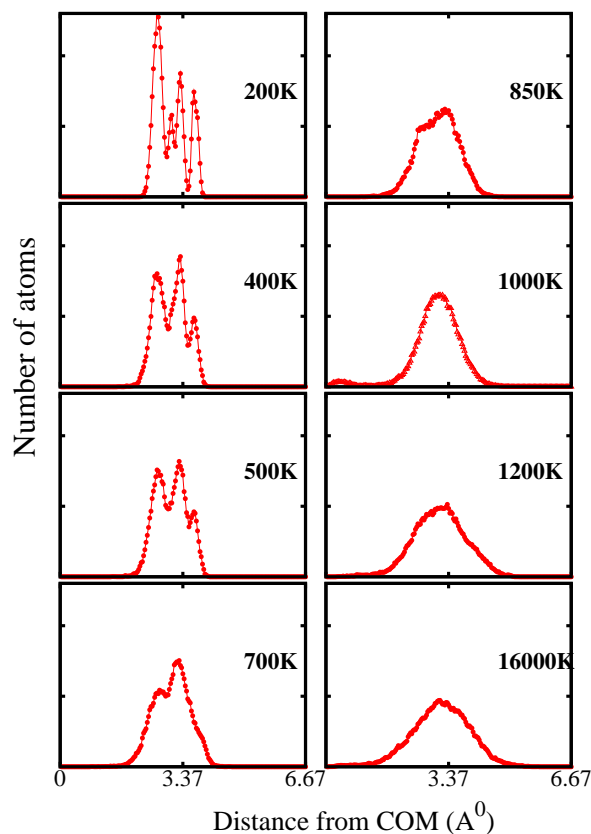
Figure 5. Radial distribution function of Au_{17}.

15 $Å^2$ as shown in figure 4. A significant observation that emerges from our studies is that the cage structure is very stable and retains its shape at least till 1000 K resulting into a heat capacity curve with relatively sharper peak.

The stability of the hollow cages can be established by calculating the radial distribution functions at various temperatures. In figure 5 we show the radial distribution function for Au_{17}. It shows three prominent peaks even up to 500 K, corresponding to the three shells indicating the existence of the cage structure. At 600 K, the three shells merge into two, indicating a diffusive motion of ions within the shell. This shell structure is retained up to 850 K. Around melting temperature, that is ≈1000 K, these two peaks are seen to merge into a single one. The figure also clearly reveals that there are no atoms within the radius of about 2.0 Å.

Now we turn to examine the isomer energy distribution (figure 6) and its influence on the specific heat. The significance and relationship between the nature of the isomer energy distribution and the shape of the heat capacity curve has been discussed by Bixon and Jortner [53]. It can be seen from figure 6 that the isomer distribution of Au_{16} is relatively continuous while Au_{17} shows a step-like structure
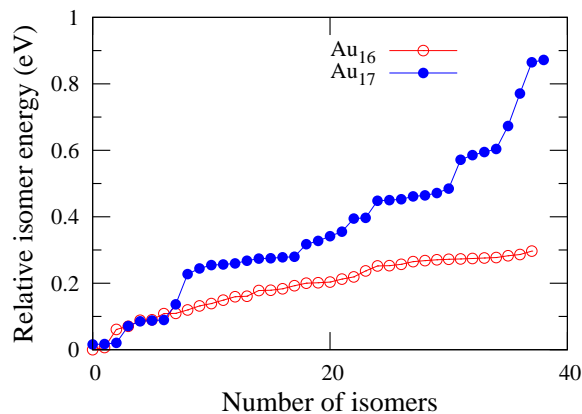
Figure 6. The distribution of isomer energies for Au_{16} and Au_{17}.

or more precisely multiple bunched level structure. As discussed by Bixon and Jortner, such a structure leads to hierarchical isomerization which is seen as a weak shoulder in the specific heat curve of Au_{17}. In the case of systems exhibiting gapless spectra (such as Au_{16}) there is no clear transition in caloric curve and that leads to a relatively broad specific heat curve. It is interesting to note that the ordered structures normally lead the isomer energy distribution having gaps. In the case of disordered ground states, a minor rearrangement of the atoms gives rise to many nearly degenerate isomers leading to an almost continuous spectrum [38,41,42].

Finally, we compare the specific heats of these two clusters with those of Au_{19} and Au_{20} [39]. It may be recalled that a highly symmetric Au_{20} cluster shows a sharp melting peak at around 770 K while Au_{19} having one vacancy (the missing apex atom of the pyramid) has a broad peak. In contrast with Au_{20} both the clusters here show rather broad specific heat curves. This is consistent with the fact that the ground state of Au_{20} is highly symmetric while both Au_{16} and Au_{17} are relatively disordered. Although Au_{19} retains the symmetry, the broad specific heat curve has been attributed to the vacancy, i.e. the absence of vertex atom.

4. Summary and conclusions

We have carried out finite temperature simulations on caged clusters of gold (Au_{16} and Au_{17}) using *ab initio* density functional molecular dynamics. Our calculations establish that the hollow cage of Au_{17} remains stable up to 1000 K whereas that of Au_{16} distorts significantly much earlier. The resulting heat capacity curves have been discussed and compared. Our results for the ground state geometry are in agreement with the earlier results and show Au_{16} to be a flat cage while Au_{17} to be hollow one. Isomer energy distribution for Au_{16} is continuous while that of Au_{17} is step-like. This leads to variation in their behaviour at finite temperature. Specific heat curve for Au_{16} has a very broad peak ranging from 600 to 1000 K whereas Au_{17} has a relatively sharper peak.

Prachi Chandrachud et al

Acknowledgements

References

[1] P J Dyson and D M P Mingos, *Gold: Progress in chemistry, biochemistry and technology* edited by H Schmidbaur (Wiley, New York, 1999) p. 511
[2] P Pyykkö, *Chem. Rev.* **88**, 563 (1988)
[3] F-R F Fan and A J Bard, *Science* **277**, 1791 (1997)
[4] J H Teles and S Brode and M Chabanas, *Angew. Chem.* **99**, 2589 (1999)
[5] M Valden, X Lai and D W Goodman, *Science* **281**, 1637 (1998)
[6] B Yoon, H Häkkinen, U Landman, A S Wörz, J-M Antonietti, S Abbet, K Judai and U Heiz, *Science* **307**, 403 (2005)
[7] F Furche, R Ahlrichs, P Weis, C Jacob, T Bierweiler and M M Kappes, *J. Chem. Phys.* **117**, 6982 (2002)
[8] H Häkkinen, B Yoon and U Landman, *J. Phys. Chem.* **A107**, 6168 (2003)
[9] X Xing, B Yoon, U Landman and J H Parks, *Phys. Rev.* **B74**, 165423 (2006)
[10] B Yoon, P Koskinen, B Huber, O Kostko, B V Issendroof, H Häkkinen, M Moseler and U Landman, *Chem. Phys. Chem.* **8**, 157 (2007)
[11] Y-K Han, *J. Chem. Phys.* **124**, 024316 (2006)
[12] J Wang, G Wang and J Zhao, *Phys. Rev.* **B66**, 035418 (2002)
[13] E M Fernandez, J M Soler, I L Garzon and L C Balbas, *Phys. Rev.* **B70**, 165403 (2004)
[14] W Fa, C Luo and J Dong, *Phys. Rev.* **B72**, 205428 (2005)
[15] P K Jain, *Struc. Chem.* **16**, 421 (2005)
[16] L Xiao, B Tollberg, X Hu and L Wang, *J. Chem. Phys.* **124**, 114309 (2006)
[17] W Fa and J Dong, *J. Chem. Phys.* **124**, 114310 (2006)
[18] S Bulusu, X Li, L-S Wang and X-C Zeng, *Proc. Natl. Acad. Sci. USA* **103**, 8326 (2006)
[19] S Bulusu and X C Zeng, *J. Chem. Phys.* **125**, 154303 (2006)
[20] X-B Li, H-Y Wang, X-D Yang, Z-H Zhu and Y-J Tang, *J. Chem. Phys.* **126**, 084505 (2007)
[21] L Xiao and L Wang, *Chem. Phys. Lett.* **392**, 452 (2004)
[22] R M Olson, S Varganov, M S Gordon, H Metiu, S Chretien, P Piecuch, K Kowalski, S A Kucharski and M Musial, *J. Am. Chem. Soc.* **127**, 1049 (2005)
[23] E M Fernandez, J M Soler and L C Balas, *Phys. Rev.* **B73**, 235433 (2006)
[24] W Fa and J Dong, *Appl. Phys. Lett.* **89**, 013117 (2006)
[25] M Ji, X Gu, X Li, X Gong, J Li and L-S Wang, *Angew. Chem. Int. Ed.* **44**, 7119 (2005)
[26] A Lechtken, D Schooss, J R Stairs, M N Blom, F Furche, N Morgner, O Kostko, B V Issendorff and M M Kappes, *Angew. Chem. Int. Ed.* **46**, 2944 (2007)
[27] L-M Wang, S Bulusu, H-J Zhai, X-C Zeng and L-S Wang, *Angew. Chem.* **46**, 2915 (2007)
[28] S Zorriasatein, K Joshi and D G Kanhere, *J. Chem. Phys.* **128**, 184314 (2008)

[29] M Schmidt, R Kusche, B von Issendorff and H Haberland, *Nature (London)* **393**, 238 (1998)
[30] M Schmidt and H Haberland, *C. R. Physique* **3**, 327 (2002)
[31] H Haberland, T Hippler, J Dongres, O Kostko, M Schmidt and B von Issendroff, *Phys. Rev. Lett.* **94**, 035701 (2005)
[32] A Shvartsburg and M F Jarrold, *Phys. Rev. Lett.* **85**, 2530 (2000)
[33] G A Breaux, R C Benirschke, T Sugai, B S Kinnear and M F Jarrold, *Phys. Rev. Lett.* **91**, 215508 (2003)
[34] G A Breaux, D A Hillman, C M Neal, R C Benirschke and M F Jarrold, *J. Am. Chem. Soc.* **126**, 8628 (2004)
[35] G A Breaux, C M Neal, B Cao and M F Jarrold, *Phys. Rev. Lett.* **94**, 173401 (2005)
[36] S Chacko, K Joshi, D G Kanhere and S A Blundell, *Phys. Rev. Lett.* **92**, 135506 (2004)
[37] S Krishnamurty, G A Breaux, S Chacko, D G Kanhere, G A Breaux, C M Neal and M F Jarrold, *Phys. Rev.* **B73**, 045406 (2006)
[38] K Joshi, S Krishnamurty and D G Kanhere, *Phys. Rev. Lett.* **96**, 135703 (2006)
[39] S Krishnamurty, G S Shafai, D G Kanhere, B Soulé de Bas and M J Ford, *J. Phys. Chem.* **A111**, 42 (2007)
[40] Mal-Soon Lee and D G Kanhere, *Phys. Rev.* **B75**, 125427 (2007)
[41] S Krishnamurty, K Joshi, S Zorriasatein and D G Kanhere, *J. Chem. Phys.* **127**, 054308 (2007)
[42] C M Neal, A K Starace, M F Jarrold, K Joshi, S Krishnamurty and D G Kanhere, *J. Phys. Chem.* **C111**, 17788 (2007)
[43] E K Yildirim and Z B Guvenc, *Modeling Simul. Mater. Sci. Eng.* **14**, 947 (2006)
[44] E K Yildirim, M Atis and Z B Guvenc, *Phys. Scr.* **75**, 111 (2007)
[45] B Soulé de Bas, M J Ford and M B Cortie, *J. Phys. Condens. Matter* **18**, 55 (2006)
[46] D Vanderbilt, *Phys. Rev.* **B41**, 7892 (1990)
[47] Vienna *ab initio* simulation package, Technische University at Wien (1999)
[48] S Nośe, *Mol. Phys.* **52**, 255 (1984)
[49] A M Ferrenberg and R H Swendsen, *Phys. Rev. Lett.* **61**, 2635 (1988)
[50] P Labastie and R L Whetten, *Phys. Rev. Lett.* **65**, 1567 (1990)
[51] D G Kanhere, A Vichare and S A Blundell, *Reviews in modern quantum chemistry* edited by K D Sen (World Scientific, Singapore, 2001)
[52] P Chandrachud, K Joshi and D G Kanhere, *Phys. Rev.* **B76**, 235423 (2007)
[53] M Bixon and J Jortner, *J. Chem. Phys.* **91**, 1631 (1989)